Eigenstructure Assignment for the Control of Highly Augmented Aircraft

Kenneth M. Sobel*
City College of New York, New York, New York
and
Frederick J. Lallman†
NASA Langley Research Center, Hampton, Virginia

Eigenstructure assignment is used to design flight control laws for aircraft with many control effectors. We show that a previous eigenstructure design for the Flight Propulsion Control Coupling aircraft lateral dynamics with three control surfaces exhibits a lack of stability robustness, due to a weak dependency relationship between the inputs. We present a method for reducing the control space to two dimensions by using the singular value decomposition. After the design is complete, we map the controller back to the original three-dimensional control space. This design approach yields a controller with both smaller gains and improved multivariable stability margins at the aircraft inputs. An interesting characteristic of the control mapping is that the most effective inputs have the larger gains, whereas the less effective inputs have smaller gains.

Introduction

EIGENSTRUCTURE assignment is an excellent method for incorporating classical specifications on damping, settling time, and mode decoupling into a modern multivariable control framework. This approach was utilized by Andry et al.[1] to design a stability augmentation system for the linearized lateral dynamics of the L-1011 aircraft. Later, Sobel and Shapiro[2] utilized eigenstructure assignment to design a pitch pointing/vertical translation control law for the linearized longitudinal dynamics of the AFTI F-16 aircraft. In Ref. 3, eigenstructure assignment is applied to the design of a yaw pointing/lateral translation control law for the linearized lateral dynamics of the Flight Propulsion Control Coupling (FPCC) aircraft. This conceptual control configured vehicle has a vertical canard in addition to the more conventional control surfaces. However, none of these designs considered eigenvalue sensitivity or multivariable stability margins.

Kautsky et al.[4] suggest that eigenstructure assignment can be used to obtain a design with eigenvalues that are least sensitive to parameter uncertainty by reducing one of several sensitivity measures. Among these measures are the quadratic norm condition number of the modal matrix and the sum of the squares of the quadratic norms of the left eigenvectors. In contrast, stability robustness of a multi-input multi-output system has been characterized by the minimum singular value of the return difference matrix at the plant input or output.[5]

In this paper, we consider the yaw pointing/lateral translation control law described in Ref. 3 for the FPCC vehicle. We show that the design is characterized by an inadequate multivariable stability margin at the plant input. We further demonstrate that minimizing the sum of squares of the eigenvalue condition numbers will result in a much degraded minimum singular value of the return difference matrix. Although the control surfaces are independent, we trace the difficulty to a weak dependency relation between the rudder, ailerons, and vertical canard. We propose a method for reducing the control space to two dimensions by using singular value decomposition.[6] After the design is complete, we map the controller back into the original three-dimensional control space. This technique yields a yaw pointing/lateral translation flight control law with excellent multivariable stability margins at the aircraft inputs.

Control Gain Design Methodology

Consider an aircraft modeled by the linear time-invariant matrix differential equation given by

$$\dot{x} = Ax + Bu \tag{1}$$

$$y = Cx \tag{2}$$

where x is the state vector ($n \times 1$), u is the control vector ($m \times 1$), and y is the output vector ($r \times 1$). Without loss of generality, we assume that the m inputs are independent and the r outputs are independent. Also, as is usually the case in aircraft problems, we assume that m, the number of inputs, is less than r, the number of outputs. If there are no pilot commands, the control vector u equals a matrix times the output vector y.

$$u = -Fy$$

The feedback problem can be stated as follows.[1] Given a set of desired eigenvalues (λ_i^d), $i = 1,2,\ldots,r$ and a corresponding set of desired eigenvectors (v_i^d), $i = 1,2,\ldots,r$, find a real $m \times r$ matrix F such that the eigenvalues of $A - BFC$ contain (λ_i^d) as a subset, and the corresponding eigenvectors of $A - BFC$ are close to the respective members of the set (v_i^d).

The feedback gain matrix F will exactly assign r eigenvalues. It will also assign the corresponding eigenvectors, provided that v_i^d is chosen to be in the subspace spanned by the columns of $(\lambda_i I - A)^{-1}B$ for $i = 1,2,\ldots,r$ as shown in Ref. 1. These subspaces are of dimension m, which is the number of independent control variables. In general, a chosen or desired eigenvector v_i^d will not reside in the prescribed subspace and, hence, cannot be achieved. Instead, a "best possible" choice for an achievable eigenvector is made. This best possible eigenvector is the projection of v_i^d onto the subspace spanned by the columns of $(\lambda_i I - A)^{-1}B$.

Received Sept. 8, 1987; revision received Jan. 27, 1988.

*Associate Professor, Department of Electrical Engineering. Associate Fellow AIAA.

†Research Engineer, Guidance and Controls Division.

Now suppose that in addition to transient shaping, we desire the controlled (or tracked) variables y_t to follow the command vector u_c with zero steady-state error where

$$y_t = Hx \tag{3}$$

The complete control law is derived by Broussard[7] and Davison.[8] If the command inputs u_c are constant, and if the tracking objective is to have the aircraft variables y_t approach the command inputs in the limit, then the control input vector is given by

$$u = (\Omega_{22} + FC\Omega_{12})u_c - Fy \tag{4}$$

where

$$\Omega = \begin{bmatrix} \Omega_{11} & \Omega_{12} \\ \Omega_{21} & \Omega_{22} \end{bmatrix} = \begin{bmatrix} A & B \\ H & O \end{bmatrix}^{-1}$$

Sensitivity and Robustness

Let the nominal closed-loop system matrix be given by

$$A_c = A - BFC \tag{5}$$

with distinct eigenvalues λ_i and corresponding eigenvectors v_i, $i = 1,2, \ldots, n$. We define the quadratic norm of a vector, denoted by $\|\cdot\|_2$, as the square root of the sum of the squares of the entries of the vector. The quadratic norm of a matrix, denoted by $\|\cdot\|_2$, is defined to be the maximum singular value of the matrix.

Let the matrix E represent a perturbation such that the perturbed closed-loop system matrix is given by $A_c + E$ with eigenvalues λ_i'; $i = 1,2, \ldots, n$. Then, as shown by Stewart[9]

$$|\lambda_i - \lambda_i'| \leqq |y_i^* E v_i| \leqq \|E\|_2 \cdot \|y_i\|_2 \tag{6}$$

where v_i, $i = 1,2, \ldots, n$ is an eigenvector of A_c normalized to unit length in the quadratic norm sense; y_i, $i = 1,2, \ldots, n$ is the corresponding left eigenvector of A_c; and $(\ )^*$ is the complex conjugate transpose.

Thus, the change in the ith eigenvalue of A_c, due to the perturbation E, is bounded above by the product of the quadratic norms of the perturbation and the ith left eigenvector. For a constant perturbation E, one can minimize this upper bound on the change in the ith eigenvalue by minimizing the quadratic norm of the left eigenvector, which is sometimes called the condition number of the ith eigenvalue. Furthermore, a bound on the eigenvalue condition numbers is given by[4,10]

$$\max_i \|y_i\|_2 \leqq \kappa_2(M) \tag{7}$$

where $\kappa_2(M)$ is the quadratic norm condition number of the normalized modal matrix. The quantities $\|y_i\|_2$ and $\kappa_2(M)$ are related by[4,10]

$$1 \leqq \kappa_2(M) \leqq n^{\frac{1}{2}} \left(\sum_i \|y_i\|_2^2 \right)^{\frac{1}{2}} \tag{8}$$

To compute the eigenvalue condition number $\|y_i\|_2$ for a complex conjugate eigenvalue pair $\lambda_{1,2} = \alpha \pm j\beta$, we let the eigenvector corresponding to λ_1 be[11]

$$v_1 = t_1 + jt_2 \tag{9}$$

Then, normalized v_1 such that

$$\|v_1\| = [t_1^T t_1 + t_2^T t_2]^{\frac{1}{2}} = 1 \tag{10}$$

Let

$$y_1^T t_1 = y_2^T t_2 = 1$$
$$y_i^T t_j = 0, \ i \neq j (i,j = 1,2) \tag{11}$$

Then, the condition number for the mode represented by $\lambda_{1,2} = \alpha \pm j\beta$ is given by[11]

$$[y_1^T y_1 + y_2^T y_2]^{\frac{1}{2}} \tag{12}$$

Finally, we review the measure that we shall use to determine stability robustness. Suppose that the modeling errors may be described by the matrix L given by

$$L = \text{diag}\,(\ell_1 e^{j\phi_1}, \ell_2 e^{j\phi_2}, \ldots, \ell_m e^{j\phi_m}) \tag{13}$$

At nominal conditions the gains $\ell_1, \ldots, \ell_m$ equal one, and phase angles $\phi_1, \ldots, \phi_m$ equal zero. The multivariable gain margin describes the range of $\ell_1, \ldots, \ell_m$ for which stability is ensured when $\phi_1, \ldots, \phi_m$ are all zero. The multivariable phase margin describes the range of $\phi_1, \ldots, \phi_m$ for which stability is ensured when $\ell_1, \ldots, \ell_m$ are all one.

The multivariable gain and phase margins at the input port have been derived by Lehtomaki.[12] Let $\sigma_{\min}\,[I + FG(s)] > \Delta$. Then, the upward gain margin is at least as large as $1/(1-\Delta)$, and the gain reduction margin is at least as small as $1/(1+\Delta)$. The phase margins are at least $\pm 2 \sin^{-1}(\Delta/2)$. For our notation, $G(s) = C(sI - A)^{-1}B$, and F is the feedback gain matrix for the control law $u = -Fy$.

Control Effector Mapping Strategy

The idea of computing a pseudocontrol with lower dimension than the true control was proposed by Lallman.[13] His pseudocontrols were computed so that each pseudocontrol has its effect concentrated upon a single selected mode by using a modal decomposition of the linearized aircraft model. Here we propose a result based upon the singular value decomposition of the control distribution matrix, denoted by B in Eq. (1). We assume that the matrix B is scaled such that all inputs are expressed in the same or equivalent units.

Consider the singular value decomposition of the matrix B given by

$$\begin{aligned} B &= U\Sigma V^T \\ &= [U_3 U_0] \begin{bmatrix} \Sigma_3 & \\ & 0 \end{bmatrix} \begin{bmatrix} V_3^T \\ V_0^T \end{bmatrix} \end{aligned} \tag{14}$$

where U is the matrix of left singular vectors, V is the matrix of right singular vectors, and Σ is a diagonal matrix containing the singular values in the order of descending magnitude.

Suppose we partition the matrix Σ_3 as follows:

$$\Sigma_3 = \begin{bmatrix} \sigma_1 & & & & & & \\ & \ddots & & & & & \\ & & \sigma_a & & & & \\ & & & \sigma_{a+1} & & & \\ & & & & \ddots & & \\ & & & & & \sigma_b \end{bmatrix} = \begin{bmatrix} \Sigma_1 & \\ & \Sigma_2 \end{bmatrix} \tag{15}$$

where

$$\sigma_b \leqq \sigma_{b-1} \leqq \cdots \leqq \sigma_{a+1} < \varepsilon$$

with ε not necessarily close to zero. If we partition U_3 and V_3 conformally with Σ_3, then we rewrite Eq. (14) as follows:

$$B = [U_1 U_2 U_0] \begin{bmatrix} \Sigma_1 & & \\ & \Sigma_2 & \\ & & 0 \end{bmatrix} \begin{bmatrix} V_1^T \\ V_2^T \\ V_0^T \end{bmatrix} \tag{16}$$

Now let the system with pseudocontrol $\boldsymbol{\delta}$ be described by

$$\dot{x} = Ax + \tilde{B}\boldsymbol{\delta} \tag{17}$$

$$y = Cx \tag{18}$$

where

$$\tilde{B} = U_1 \tag{19}$$

We design a feedback (and possibly a feedforward) pseudocontrol $\boldsymbol{\delta}$ for the system described by Eqs. (17)–(19). Then, the true control $\boldsymbol{u}$ for the system described by Eqs. (1) and (2) is given by

$$\boldsymbol{u} = V_1 \Sigma_1^{-1} \boldsymbol{\delta} \tag{20}$$

To derive the inverse control mapping given by Eq. (20), we observe that upon comparing Eqs. (1) and (17), we require

$$B\boldsymbol{u} = \tilde{B}\boldsymbol{\delta} \tag{21}$$

Solving for the true control u, we obtain

$$\boldsymbol{u} = B^{+}\tilde{B}\boldsymbol{\delta} \tag{22}$$

where the pseudoinverse B^{+} may be written as[6]

$$B^{+} = V_3 \Sigma_3^{-1} U_3^T \tag{23}$$

Upon combining Eqs. (19), (22), and (23) we obtain

$$\boldsymbol{u} = (V_3 \Sigma_3^{-1} U_3^T)U_1\boldsymbol{\delta} \tag{24}$$

Using Eq. (16) yields

$$\boldsymbol{u} = [V_1 V_2]\begin{bmatrix} \Sigma_1^{-1} & \\ & \Sigma_2^{-1} \end{bmatrix}\begin{bmatrix} U_1^T \\ U_2^T \end{bmatrix} U_1\boldsymbol{\delta} \tag{25}$$

Expand Eq. (25) to obtain

$$\boldsymbol{u} = V_1 \Sigma_1^{-1} U_1^T U_1\boldsymbol{\delta} + V_2 \Sigma_2^{-1} U_2^T U_1\boldsymbol{\delta} \tag{26}$$

But, from the properties of the singular value decomposition,[6] we have that U and V are unitary matrices. Hence

$$U_1^T U_1 = I \tag{27}$$

and

$$U_2^T U_1 = 0 \tag{28}$$

Thus, we obtain the desired result that

$$\boldsymbol{u} = V_1 \Sigma_1^{-1} \boldsymbol{\delta} \tag{29}$$

We remark that the computation of the true control $\boldsymbol{u}$ only requires the inversion of a diagonal matrix. Furthermore, if the pseudocontrol gains have reasonable magnitudes, then the gains in the true control law u will also have reasonable magnitudes. This is because the matrix Σ_1^{-1} in Eq. (20) only contains the recriprocals of the singular values that we did not consider to be too small. If the pseudocontrol strategy is not utilized, then the eigenstructure assignment feedback gains would be a function of the matrix Σ_3^{-1}, as shown in Ref. 4. This matrix would have some large diagonal entries that will yield gains with large magnitudes. Thus, the key to the pseudocontrol strategy is to discard the small, but not necessarily near zero, singular values of the matrix B. This is equivalent to not using the control in the directions of least control effectiveness. Finally, we should indicate that use of the pseudocontrol strategy is not limited to feedback gains designed by utilizing eigenstructure assignment. Lallman[13] has used a related pseudocontrol strategy based upon a modal decomposition in conjunction with feedback gains computed via the linear quadratic regulator approach.

FPCC Flight Control Design

Consider the fifth-order FPCC aircraft linearized lateral dynamics described by

$$\frac{\mathrm{d}}{\mathrm{d}t}\begin{bmatrix} \beta \\ \phi \\ p \\ r \\ \gamma \end{bmatrix} = \begin{bmatrix} -0.340 & 0.0517 & 0.001 & -0.997 & 0 \\ 0 & 0 & 1 & 0 & 0 \\ -2.69 & 0 & -1.15 & 0.738 & 0 \\ 5.91 & 0 & 0.138 & -0.506 & 0 \\ -0.340 & 0.0517 & 0.001 & 0.0031 & 0 \end{bmatrix}\begin{bmatrix} \beta \\ \phi \\ p \\ r \\ \gamma \end{bmatrix} + \begin{bmatrix} 0.0755 & 0 & 0.0246 \\ 0 & 0 & 0 \\ 4.48 & 5.22 & -0.742 \\ -5.03 & 0.0998 & 0.984 \\ 0.0755 & 0 & 0.0246 \end{bmatrix}\begin{bmatrix} \delta_r \\ \delta_a \\ \delta_c \end{bmatrix} \tag{30}$$

The state variables are sideslip angle β, bank angle ϕ, roll rate p, yaw rate r, and lateral/directional flight-path angle $(\gamma = \psi + \beta)$, where ψ is the heading angle. The control variables are rudder δ_r, ailerons δ_a, and vertical canard δ_c. The angles and surface deflections are in degrees, and the angular rates are in degrees per second. The five measurements are β, ϕ, p, r, γ. This model is identical to the one utilized in Ref. 3, with the actuator dynamics neglected for simplicity. We remark that the minimum nonzero singular value of the matrix B in Eq. (30) is given by

$$\sigma_{\min}(B) = 0.0546$$

and the quadratic norm condition number of the matrix B is given by

$$\sigma_{\max}(B)/\sigma_{\min}(B) = 144.614$$

Thus, it is reasonable to conclude that the matrix B has full rank and the control inputs are independent.

The design goal is a yaw pointing/lateral translation control law in which the lateral/directional flight-path response is decoupled from the yaw rate response. In addition, both of these responses should be decoupled from the roll rate and bank angle response. From Ref. 3, the desired eigenvalues and eigenvectors are

dutch roll mode:

$$\lambda_{\mathrm{dr}}^{\mathrm{d}} = -2 \pm j2 \tag{31a}$$

roll mode:

$$\lambda_{\mathrm{roll}}^{\mathrm{d}} = -3 \pm j2 \tag{31b}$$

flight-path mode:

$$\lambda_5^{\mathrm{d}} = -0.5 \tag{31c}$$

$$\boldsymbol{v}_{\mathrm{dr}}^{\mathrm{d}} = \begin{bmatrix} x \\ 0 \\ 0 \\ 1 \\ 0 \end{bmatrix} \pm j \begin{bmatrix} 1 \\ 0 \\ 0 \\ x \\ 0 \end{bmatrix} \quad \boldsymbol{v}_{\mathrm{roll}}^{\mathrm{d}} = \begin{bmatrix} 0 \\ x \\ 1 \\ 0 \\ 0 \end{bmatrix} \pm j \begin{bmatrix} 0 \\ 1 \\ x \\ 0 \\ 0 \end{bmatrix} \quad \boldsymbol{v}_5^{\mathrm{d}} = \begin{bmatrix} x \\ 0 \\ 0 \\ 0 \\ 1 \end{bmatrix} \tag{32}$$

The eigenstructure assignment feedback gain matrix (f_{ij}) is shown in Table 1, and some measures that can be used to evaluate the design are shown in Table 2. We observe that the quadratic norm condition number of the modal matrix is moderate, which indicates that the design should exhibit acceptable eigenvalue sensitivity. However, the norm of the feedback gain matrix may be considered large. We remark that the largest feedback gains are in the canard loop, which is the least effective of the control surfaces. Furthermore, the minimum singular value of the return difference matrix at the inputs is only 0.18, which corresponds to a gain margin of [−1.44 dB, 1.72 dB] and a phase margin of 10.33 deg. We compute feedforward gains based upon a command vector $u_c = [\psi_c \gamma_c \phi_c]^T$, which is allowable because we have three inputs and, therefore, we can command three tracked variables. Thus, we will command a step in either heading angle or lateral flight-path angle while always commanding bank angle to be zero. The feedforward gains that would multiply either a heading or lateral flight-path command are shown in Table 1. The achievable eigenvectors are shown in Table 3 from which we observe that the couplings between the dutch roll mode and flight-path response, roll mode and flight-path response, and flight-path mode and yaw rate response are all very small. Hence, we expect that the yaw pointing and lateral translation performance objectives have been achieved. This is verified by the time responses that are shown in Figs. 1a and 1b for a heading command and lateral flight-path command, respectively. Because of the choice of feedforward gains, the design achieves zero steady-state error to a unit step command. We remark that the transient canard deflection is approximately 9 deg from its steady-state value for yaw pointing, and approximately 6 deg from its steady-state value for lateral translation. Hence, the feedback control law is causing hefty canard deflection for a 1 deg command. Later, when we describe the pseudocontrol design, we will observe that although a large steady-state canard deflection is required for the tracking objective, only a small transient canard deflection is caused by the feedback control law. Thus, while the initial design is relying heavily on the ineffective canard for stability, the pseudocontrol design will rely heavily on the more effective rudder and ailerons for stability.

Kautsky et al.[4] suggest that minimizing the eigenvalue condition numbers when using full state feedback is a desirable design goal. Therefore, we choose to minimize the sum of the squares of the eigenvalue condition numbers subject to the eigenvalue assignment of Eq. (31). Mathematically,

$$\text{minimize } [\,\|y_{\mathrm{d}r}\|_2^2 + \|y_{\mathrm{roll}}\|_2^2 + \|y_5\|_2^2] \tag{33}$$

subject to

$$\lambda_{\mathrm{d}r}^{\mathrm{d}} = -2 \pm j2$$

$$\lambda_{\mathrm{roll}}^{\mathrm{d}} = -3 \pm j2$$

$$\lambda_5^{\mathrm{d}} = -0.5$$

where the eigenvalue condition numbers in Eq. (33) are defined by Eqs. (5), (6), and (9)–(12).

Each closed-loop eigenvector can be written as

$$v_i = L_i z_i \tag{34}$$

where

$$L_i = (\lambda_i I - A)^{-1} B \tag{35}$$

Thus, with the eigenvalues specified, each closed-loop eigenvector is parameterized by the vector z_i. For our example, $z_{\mathrm{d}r}$ and z_{roll} are (10×1) vectors, and z_5 is a (5×1) vector. Here we are performing all computations using real arithmetic. We perform the optimization in Eq. (33) over the space consisting of the entries of $z_{\mathrm{d}r}$, z_{roll}, and z_5. We choose to utilize IMSL subroutine ZXMWD[14] to perform a quasi-Newton optimization. This subroutine chooses 100 points in a user-specified region and performs four iterations on each point. Then, an optimization to convergence is performed on the five points that have the smallest objective function value after the initial four iterations. To allow the 100 points to be chosen over some large region, we arbitrarily limit each entry of $z_{\mathrm{d}r}$, z_{roll}, and z_5 to have magnitude less than or equal to 50. We believe that utilizing any larger region will yield the same solution. In any case, this optimization yields a solution with both reduced eigenvalue condition numbers and smaller quadratic norm condition number of the closed-loop modal matrix as compared to the previous design.

The feedback gain matrix for this minimum sensitivity design is shown in Table 1, and some measures that can be used to evaluate the design are shown in Table 2. We observe that although the eigenvalue sensitivity measures have been reduced, the magnitude of the feedback gains is unacceptably

Table 1 FPCC gain matrices

Design	Feedback gain matrix β	ϕ	p	r	γ	Feedforward gain matrix			
Initial	−1.45	0.287	−0.000618	−0.410	1.50	−0.978	2.48		
	−0.604	2.42	0.935	0.690	0.942	1.27	−0.324		
	−9.39	1.22	0.0425	1.38	15.7	3.00	12.71		
Minimum sensitivity	7.30	0.275	−0.00528	−9.28	4.77	−9.72	14.5		
	−0.649	1.47	0.558	1.78	−0.172	1.31	−1.48		
	43.2	1.26	0.0569	−44.6	27.6	−49.5	77.2		
						Pseudocontrols		Original controls	
Pseudocontrol	0.547	0.0306	−0.0084	−0.712	−2.85				
	−1.01	2.47	0.940	0.788	2.62	−1.82	−1.03	−2.96	0.113
	−0.132	0.0565	0.0254	0.159	0.622	−10.98	13.59	1.66	0.956
						0.0775	0.545	−6.28	6.91

Table 2 FPCC Control law comparison

Design	$(\Sigma\|y_i\|^2)^{\frac{1}{2}}$	$\kappa_2(M)$	$\inf \sigma_{\min}(I + FG)$	$(\Sigma f_{ij}^2)^{\frac{1}{2}}$
Initial	9.45	7.48	0.18	18.74
Minimum sensitivity	5.28	5.11	0.025	69.19
Pseudocontrol	10.79	12.1	0.9835	4.98

Table 3 FPCC Achievable eigenvector comparison

Design	Dutch roll mode Real	Dutch roll mode Imaginary	Roll mode Real	Roll mode Imaginary	Flight-path mode	
Initial	3.26×10^{-1}	7.59×10^{-2}	9.07×10^{-6}	-8.36×10^{-5}	7.12×10^{-1}	β
	3.53×10^{-4}	7.69×10^{-4}	2.58×10^{-1}	6.88×10^{-2}	1.81×10^{-4}	ϕ
	-2.23×10^{-3}	-8.37×10^{-4}	-9.12×10^{-1}	3.11×10^{-1}	-9.05×10^{-5}	p
	-8.02×10^{-1}	-4.94×10^{-4}	-1.36×10^{-4}	-2.67×10^{-4}	4.75×10^{-3}	r
	-4.71×10^{-5}	-3.55×10^{-5}	-6.39×10^{-7}	-1.18×10^{-6}	7.02×10^{-1}	γ
Pseudocontrol	-3.40×10^{-1}	-6.35×10^{-2}	1.89×10^{-3}	1.72×10^{-3}	-8.66×10^{-1}	β
	2.16×10^{-5}	8.17×10^{-4}	-2.59×10^{-1}	-6.83×10^{-2}	1.47×10^{-2}	ϕ
	-1.67×10^{-3}	-1.59×10^{-3}	9.12×10^{-1}	-3.10×10^{-1}	-7.33×10^{-3}	p
	-7.19×10^{-1}	6.02×10^{-1}	-2.83×10^{-3}	-2.42×10^{-3}	-2.05×10^{-1}	r
	-9.86×10^{-3}	-3.44×10^{-2}	2.17×10^{-3}	2.71×10^{-3}	-4.55×10^{-1}	γ

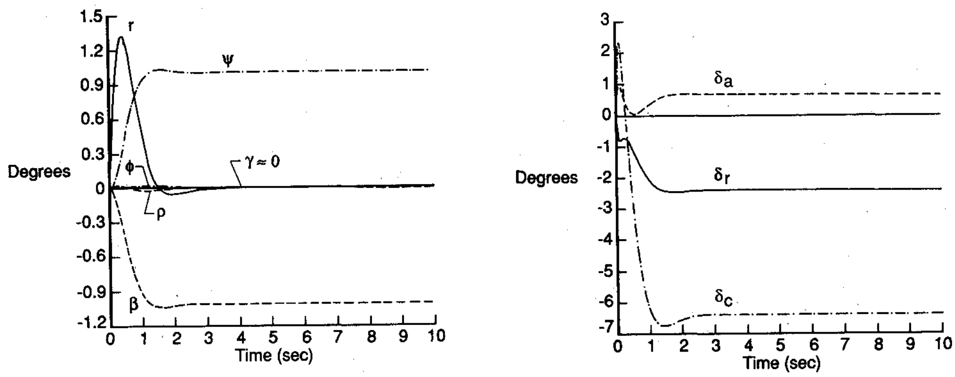

Fig. 1a FPCC initial design—heading command.

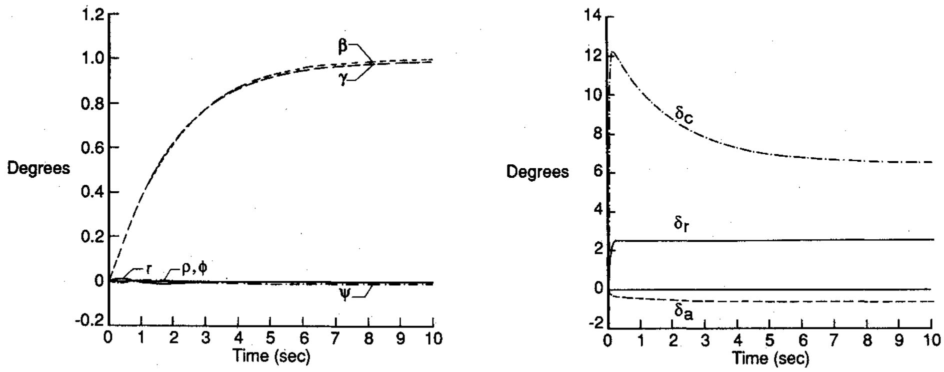

Fig. 1b FPCC initial design—lateral flight-path command.

large. The largest gains are in the canard loop, which is the least effective control surface. In fact, the canard deflection saturates in less than 0.1s in response to a unit step command. Unit step commands in heading angle and lateral flight-path angle produce canard deflections of -41 deg and $+70$ deg respectively. Finally, this design exhibits an extreme lack of stability robustness as measured by the minimum singular value of the return difference matrix at the inputs. For this design, $\sigma_{\min}(I + FG) = 0.025$, which corresponds to a gain margin of $[-0.21 \text{ dB}, 0.22 \text{ dB}]$ and a phase margin of ± 1.43 deg. If we compute stability margins for each loop, we find that the β/δ_r loop exhibits a gain margin of 1.8 dB and a phase margin of 15 deg. Of course, these later numbers assume that there is no uncertainty in any of the other loops.

Finally, we consider a design based upon mapping the rudder, ailerons, and canard into a two-dimensional pseudocontrol vector. The singular values of the control distribution matrix B are

$$\sigma_1 = 7.8959, \qquad \sigma_2 = 3.4504, \qquad \sigma_3 = 0.0546, \qquad \sigma_4 = \sigma_5 = 0$$

and the matrix of corresponding left singular vectors is given by

$$U = \begin{array}{c@{}c} \left[\begin{array}{ccccc} 0.0074 & -0.0109 & 0.7070 & 0.2461 & -0.6629 \\ 0 & 0 & 0 & 0.9375 & 0.3481 \\ 0.8455 & 0.5340 & -0.0006 & 0 & 0 \\ -0.5339 & 0.8453 & 0.0186 & 0 & 0 \\ 0.0074 & -0.0109 & 0.7070 & -0.2461 & 0.6629 \end{array}\right] & \begin{array}{c} \beta \\ \phi \\ p \\ r \\ \gamma \end{array} \end{array}$$

We observe that the first two singular vectors that correspond to the two largest singular values distribute the control to primarily effect rolling and yawing moments. The singular vector corresponding to the small singular value distributes the control to primarily effect side-force and lateral flight-path rate. These quantities are difficult to control directly as indicated by the small value of σ_3. Any attempt to do so, without some constraint on control gain magnitudes, would result in large gains as evidenced by the initial control design. Finally, the last two singular vectors that correspond to zero singular values attempt to directly control ϕ, which is not possible because the second row of the matrix B contains all zero entries. We choose the columns of the new control distribution matrix $\tilde{B}$ to be the first two singular vectors, and we compute a control law for the system described by Eqs. (17) and (18). The desired eigenvalues and desired eigenvectors are given, as before, by Eqs. (31) and (32). However, now the achievable eigenvectors will not be as close to the desired eigenvectors (in the quadratic norm sense) because we have only two pseudocontrols. That is, we are now projecting the desired eigenvectors onto two-dimensional subspaces, as compared to the three-dimensional subspaces in the previous design.

The control gains for the actual control law, which are obtained via the inverse mapping given by Eq. (20), are shown in Table 1 for this new pseudocontrol design. Once again some figures of merit are shown in Table 2. We observe that the eigenvalue condition numbers are larger than the initial design. However, the norm of the feedback gain matrix is approximately one-fourth of the norm for the initial design. Furthermore, the minimum singular value of the return difference matrix at the inputs is given by $\sigma_{\min}(I+FG)=0.9835$. This corresponds to multivariable gain margins of [−5.9 dB, 35.65 dB] and a phase margin of ±58.91 deg. Thus, we have achieved excellent multivariable stability margins and significantly smaller feedback gains at the expense of an increase in the eigenvalue sensitivity measures. Furthermore, the smallest feedback gains are in the canard loop. The feedback control is now relying heavily on the rudder and ailerons for stability. This is in contrast to the previous designs where the controller relied heavily on the ineffective canard for stability.

The closed-loop eigenvectors for the pseudocontrol design are shown in Table 3. We observe that the eigenvector entries that distribute the dutch roll mode to the flight-path response are small, but larger than the initial design. Thus, we expect that a heading command, which excites the dutch roll mode, will cause a transient flight-path response that is small, yet larger than the initial design. In contrast, the eigenvector entry that distributes the flight-path mode to the yaw rate response is considered to be moderately large for the pseudocontrol design. Thus, we expect that a flight-path command may cause a significant transient in yaw rate and heading angle. Therefore, the yaw pointing control should be excellent, but the lateral translation control may exhibit a significant transient in heading angle. This may be a physical limitation caused by the size and location of the vertical canard.

Next, we consider the computation of feedforward gains that yield zero steady-state error to a step command in either heading angle or lateral flight-path angle. One possible approach is to compute feedforward gains that couple the heading and flight-path commands to the pseudocontrols. Then, these gains could be inverse mapped via Eq. (20) to obtain the feedforward gains that couple the commands to the actual control surfaces. Feedforward gains computed by using this approach are shown in Table 1 under the pseudo controls heading. We observe that the larger gains couple the commands to the rudder and ailerons, whereas smaller gains couple the commands to the canard. Time responses of this design indicate that significant rolling motion occurs in response to a step command in either heading or flight path. This is because with only two pseudocontrols we can only command two tracked variables. Hence, we cannot command a step in heading while commanding both flight path and bank angle to be zero. Alternatively, we cannot command a step in flight path while commanding both heading and bank angle to be zero.

To achieve the tracking objectives, we directly compute feedforward gains that couple the heading, flight path, and bank angle commands to the rudder, ailerons, and canard. Thus, we use the pseudocontrol strategy to compute the feedback gains, but not the feedforward gains. These new feedforward gains are shown in Table 1 under the original controls heading. The feedforward gains that couple bank angle command to the three control surfaces are not shown because bank angle will always be commanded to be zero. We observe that the larger feedforward gains now couple the commands to the canard. Thus, a large steady-state canard deflection is required in order to achieve the tracking objective.

Time responses for unit step commands in heading angle and lateral flight-path angle are shown in Figs. 2a and 2b, respectively. As expected, the yaw pointing task is achieved with only

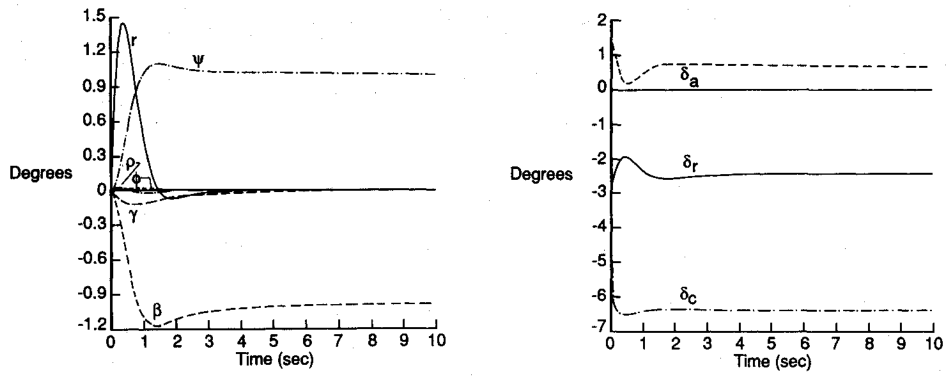

Fig. 2a FPCC pseudocontrol design—heading command.

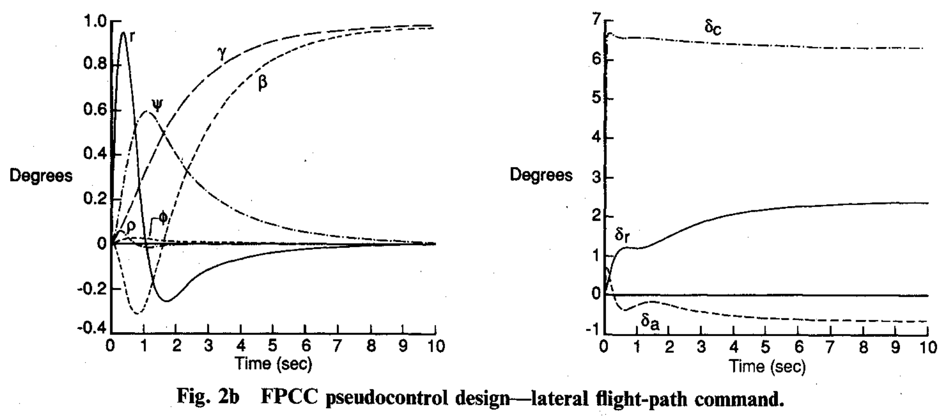

Fig. 2b FPCC pseudocontrol design—lateral flight-path command.

a small transient in the lateral flight-path angle. Also, as expected, the lateral translation task requires a moderate transient in the heading angle. We observe that large steady-state canard deflections are required to achieve these difficult specialized tasks. However, the transient canard deflections in response to unit step heading and flight-path commands are only 0.2 deg and 0.4 deg from their steady-state values, respectively. Thus, the feedback loops are only causing small canard deflections, whereas the feedforward gains are causing large steady-state canard deflections. This is in contrast to the previous designs without the pseudocontrol feedback strategy, where the feedback system caused large transient canard deflection that resulted in a lack of stability robustness.

Conclusions

We have applied eigenstructure assignment to the design of control laws for an aircraft that is augmented with a vertical canard in addition to the more conventional control surfaces. These types of augmented vehicles may exhibit a dependency relationship between the inputs that can cause large feedback gains and a lack of multivariable stability robustness. We have presented a control mapping strategy, based upon the singular value decomposition, which yields a pseudocontrol vector of lower dimension than the actual control vector. This mapping strategy was combined with eigenstructure assignment to design a yaw pointing/lateral translation control law for a specific aircraft. This new approach yields smaller feedback gains and improved multivariable stability margins as compared to an earlier design. An interesting characteristic of the control mapping strategy is that the most effective control inputs have the larger feedback gains, and the less effective control inputs have smaller feedback gains. Thus, the control inputs that are most effective are given the most emphasis in the feedback control law.

Acknowledgment

This work was partially supported by a NASA/ASEE Summer Faculty Fellowship.

References

[1]Andry, A. N., Shapiro, E. Y., and Chung, J. C., "Eigenstructure Assignment for Linear Systems," *IEEE Transactions on Aerospace and Electronic Systems*, Vol. AE-19, Sept. 1983, pp. 711–729.

[2]Sobel, K. M. and Shapiro, E. Y., "A Design Methodology for Pitch Pointing Flight Control Systems," *Journal of Guidance, Control, and Dynamics*, Vol. 8, No. 2, March–April 1985, pp. 181–187.

[3]Sobel, K. M. and Shapiro, E. Y., "Application of Eigensystem Assignment to Lateral Translation and Yaw Pointing Flight Control," *Proceedings of the 23rd IEEE Conference on Decision and Control*, Las Vegas, NV, Dec. 1984, pp. 1423–1428.

[4]Kautsky, J., Nichols, N. K., and Van Dorren, P., "Robust Pole Assignment in Linear State Feedback," *International Journal of Control*, Vol. 41, No. 5, 1987, pp. 1129–1155.

[5]Doyle, J. C. and Stein, G., "Multivariable Feedback Design: Concepts for a Classical/Modern Synthesis," *IEEE Transactions on Automatic Control*, Vol. AC-26, Feb. 1981, pp. 4–16.

[6]Klema, V. C. and Laub, A. J., "The Singular Value Decomposition: Its Computation and Some Applications," *IEEE Transactions on Automatic Control*, Vol. AC-25, No. 2, April 1980, pp. 164–176.

[7]O'Brien, M. J. and Broussard, J. R., "Feedforward Control to Track the Output of a Forced Model," *Proceedings of the 17th IEEE Conference on Decision and Control*, San Diego, CA, Jan. 1979, pp. 1149–1155.

[8]Davison, E. J., "The Steady State Invertibility and Feedforward Control of Linear Time Invariant Systems," *IEEE Transactions on Automatic Control*, Vol. AC-21, No. 4, Aug. 1976, pp. 529–534.

[9]Stewart, G. W., *Introduction to Matrix Computations*, Academic, New York, 1973.

[10]Wilkinson, J. H., *The Algebraic Eigenvalue Problem*, Oxford Univ. Press, Oxford, 1965.

[11]Srinathkumar, S. and Jategaonkar, R. V., "Robust Eigensystem Assignment in Multi-Input Systems," National Aeronautical Lab., Bangalore, India, TM SE8506, May 1985.

[12]Lehtomaki, N. A., "Practical Robustness Measures in Multivariable Control System Analysis," Ph.D. Thesis, Massachusetts Inst. of Technology, Cambridge, MA, May 1981.

[13]Lallman, F. J., "Relative Control Effectiveness with Application to Airplane Control," NASA TP-2416, April 1985.

[14]*IMSL Reference Manual,* 9th ed., IMSL, Inc., Houston, TX, 1982.